Synthesis and Structure of Arene Ru(II) N ∧ O-Chelating Complexes: In Vitro Cytotoxicity and Cancer Cell Death Mechanism

Sundarraman Balaji, Mohamed Kasim Mohamed Subarkhan, Hangxiang Wang, Rengan Ramesh, David Semeril

Synthesis and structural elucidation of half-sandwich arene Ru(II) benzhydrazone complexes : Antiproliferative activity and cell death mechanism

Sundarraman Balaji[a] Mohamed Kasim Mohamed Subarkhan[b] Hangxiang Wang[b] Rengan Ramesh[a*] David Semeril[c]

[a]Centre for Organometallic Chemistry, School of chemistry, Bharathidasan University, Tiruchirappalli- 620 024, Tamil Nadu, India.

[b]The First Affiliated Hospital; Key Laboratory of Combined Multi-Organ Transplantation, Ministry of Public Health, School of Medicine, Zhejiang University, Hangzhou, 310003, PR China.

[c]Laboratoire de Chimie Inorganique et Catalyse, Institut de Chimie, Universite de Strasbourg, UMR 7177, CNRS, France.

Correspondence

Centre for Organometallic Chemistry, School of Chemistry, Bharathidasan University, Tiruchirappalli 620 024, Tamil Nadu, India. Email: rramesh@bdu.ac.in

ABSTRACT

A panel of six new structurally related half-sandwich arene Ru(II) complexes of the type [Ru(**L**)Cl(η^6-arene)] (**L** = dimethylaminobenzhydrazones; arene = benzene or *p*-cymene) were synthesized, in search of new ruthenium anticancer drugs. The formation of the complexes has been completely characterized by elemental analysis and spectral (FT-IR, UV–vis, NMR and HR-MS) methods. Single crystal X-ray diffraction analysis showed that the benzhydrazone ligands were coordinated to ruthenium through imine nitrogen and imidolate oxygen and thus constituted a three legged-piano stool pseudo-octahedral structure with a support of a terminal chloride. Further, human cancer cell growth inhibition properties of the complexes have been unveiled with the aid of MTT assay against A549 (Lung carcinoma), LoVo (Colon adenocarcinoma) and HuH-7 (Hepato cellular carcinoma) cells with the standard drug cisplatin. Interestingly, complexes **4**, **5** and **6** which contain *p*-cymene moiety were found to surpass the activity of cisplatin in all the cancer cells tested and complex **6** was a topnotcher. The capacity corresponding to the inhibition of A549 cells

proliferation was analyzed by Edu assay and indicated a notable effect of the *p*-cymene counterparts **4**, **5** and **6** over cisplatin. Further examinations of the cell death mechanism signified that the anticancer activity was accomplished by inducing apoptosis in cancer cells, suggesting that these complexes are also one of the propitious candidates for cancer therapy and deserve further investigation.

Keywords:

benzhydrazones, cell death mechanism, *in vitro* cytotoxicity, Ru(II) arene complexes

1. Introduction

GLOBOCAN estimates 36 types of cancers in 185 countries based on the incidence, mortality and prevalence in the year 2018. Nowadays, chemotherapy is the most widely used cancer treatment among radio, immune, hormone and gene therapies.[1] Though metal-based anticancer drug cisplatin and its derivatives are efficacious against the various types of cancers, they produce non-cancer cell toxicity that leads to severe adverse effects, including peripheral neuropathy, hair loss and myelotoxicity in patients.[2] Owing to this unsatisfactory treatment of platinum based drugs in the scenario of undesirable side effects, scientists search non-platinum metal based drugs with target specificity, less toxicity and potent activity against a wide assortment of cancers.[3] In the examination of novel anticancer drugs, great interests have been raised on ruthenium complexes and are being tested on several cancer cells still today.[4-6]

Ruthenium compounds have desired properties that make its scaffolds, an attractive alternative for medicinal application in place of Pt counterparts by following rationales. (i) Effective towards some cisplatin resistant cancers.[7] (ii) Highly selective towards cancer cells/targets and minimal side effects (iii) Mimetic of iron in binding targets.[8] Moreover, ruthenium based drugs **KP1019**,[9] **NAMI-A**[10] have crossed clinical trials and other ruthenium drugs **KP1339**,[11] **TLD-1433**,[12] **RM175**,[13] **RAPTA-C**[14] and **RAED**[15] are under (pre)clinical studies (Figure 1). Because of the structural diversity in ancillary ligands and easy accessibility on hydrophobic nature of arenes, half-sandwich organometallic low-spin d^6 metal complexes have attracted great interest in cancer metallotherapeutics.[16] Intense investigations were focused on ligands selection from arene, phosphine and other multidentate ligands containing oxygen, nitrogen and sulphur.[17-20]

Schiff bases can coordinate to metal centres and exhibit different coordination modes which lead to the synthesis of many homo and hetero metallic complexes with varied stereochemistry found suitable for modelling active sites in biological systems.[21] Amongst Schiff bases, the benzhydrazone ligands contain an acid-labile bond resulting from the conjugation of a hydrazine moiety to a carbonyl group can be used to deliver drugs based on the relative acidic environment of tumours.[22] Metal hydrazone complexes can have a wide range of structures with different coordination numbers and geometries, accessible redox states and thermodynamic tenability operating a direct influence on biological activities.[23] Furthermore, ruthenium hydrazones have notable evidences and significances in biological activities as anticancer, antitumor, antifungal, antibacterial, antimicrobial, antioxidant agents, herbicides, insecticides, plant stimulants and also in natural oxygen carriers.[19, 24-26] In addition, the compounds possessing *p*-dimethylaminophenyl moiety exhibit noteworthy bioactivities.[27,28] So it would be interesting to construct a benzhydrazone from 4-dimethylamino benzaldehyde and benzhydrazide with various substituents to chelate arene ruthenium centre.

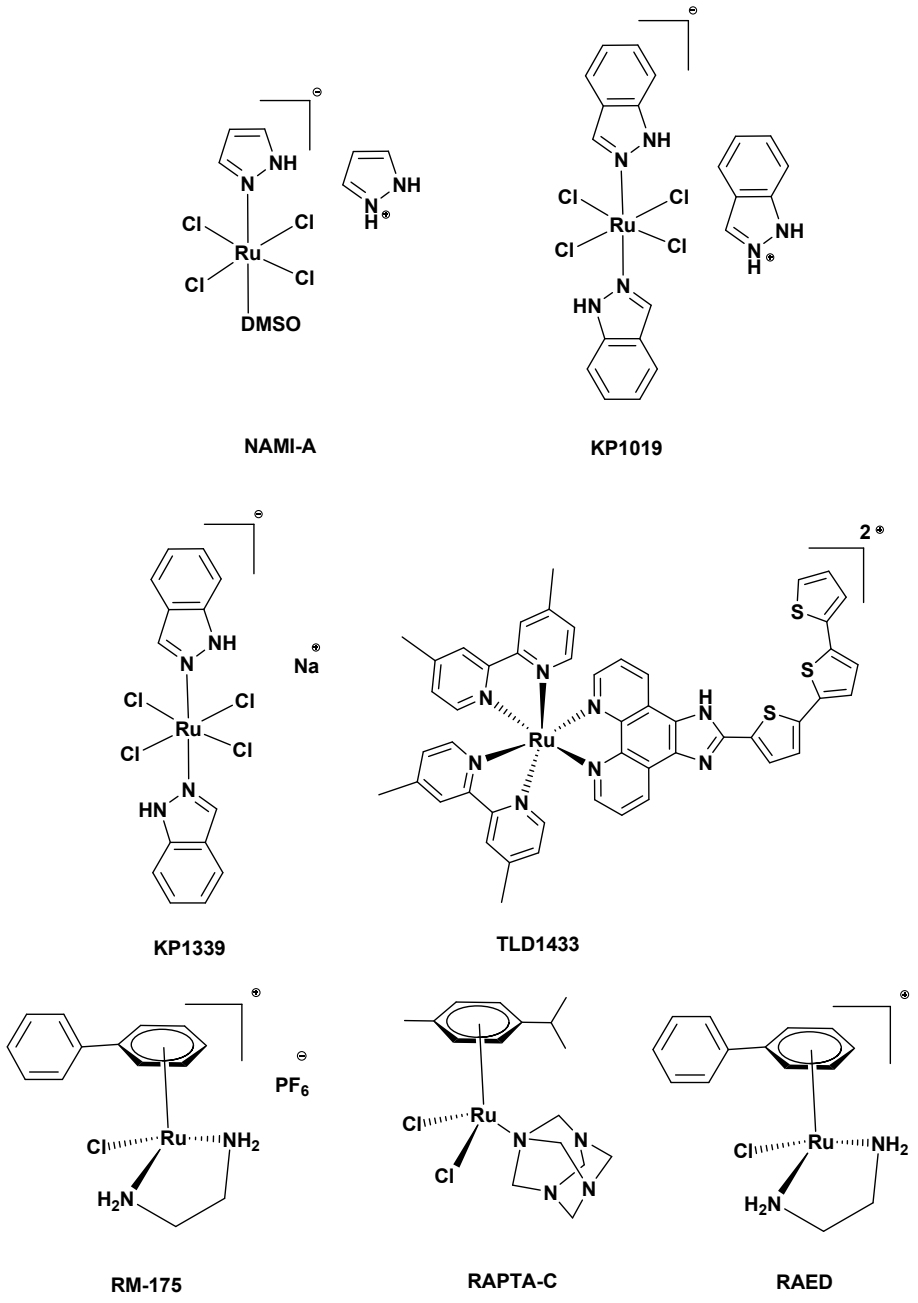

Figure 1. Structures of some ruthenium clinical, preclinical and lead anticancer complexes

Since ruthenium complexes containing benzhydrazones are emerging antiproliferative compounds, we have focused our attention to synthesize and structurally characterize a sequence of arene Ru(II) complexes containing different N'-(4 (dimethylamino)benzylidene)benzhydrazide. Prompted by the progress of ruthenium drugs in cancer chemotherapy, the titled complexes were subjected to *in vitro* anti-cancer activity studies.

2. Experimental section

Materials, methods and crystal data collection were given in supplementary information (ESI, S2).

Preparation of dimethylamino benzoylhydrazone ligands

The *p*-dimethylaminobenzaldehyde benzhydrazone ligands were prepared by stirring an ethanolic mixture (25 ml) of 4-substituded benzhydrazides (0.1mol) and *p*-dimethylaminobenzaldehyde (0.1mol) at ambient temperature. After 6 h, the completion of reaction resulted the formation of solid benzhydrazone ligands which was collected by filtration, washed with use of ethanol then dried under vacuum. Analytically pure compounds were procured from recrystallisation from methanol. Spectral data for the ligands **1-3** were given in supplementary information (ESI, S3).

Synthesis of arene Ru(II) benzhydrazone complexes

0.5 mmol of $[(\eta^6\text{-arene})RuCl_2]_2$ (arene: benzene or *p*-cymene) precursor, 1 mmol of N,N-dimethylamino benzhydrazone ligand and 1 mmol of triethylamine in 20 ml of benzene was blended and stirred for 5 h at ambient temperature. The progression of reaction was monitored through thin layer chromatography and column chromatographic separations of the reaction mixture afforded complexes **1-6** in 70:30 % of hexane:ethyl acetate eluent**.**

[Ru(L1)(η^6-C_6H_6)Cl] (**1**). Brown solid. Yield = 75%; m.p.: 185 °C (with decomposition); calculated: $C_{22}H_{22}N_3OClRu$: C, 54.22; H, 4.64; N, 8.72%. Found: C, 54.25; H, 4.61; N, 8.74%. IR (KBr, cm^{-1}): 1524 $\nu_{(C=N-N=C)}$, 1343 $\nu_{(C-O)}$, UV-Vis (CH_3CN, λ_{max}/nm) (ε_{max}/dm^3 mol^{-1} cm^{-1}): 383(1733), 292(6342), 230(14950). ^{1}H NMR (400 MHz, $CDCl_3$) (δ ppm): 8.88 (s, 1H, HC=N), 6.76–8.10 (m, 9H, Ar-H of ligand), 5.44 (s, 6H, CH-benzene), 3.08 (s, 6H, $N(CH_3)_2$). ^{13}C NMR (100 MHz, $CDCl_3$, δ, ppm): 173.31 (C─O), 160.93 (C═N), 151.71 (C-$N(CH_3)_2$), 132.30, 132.07, 130.19, 128.60, 127.85, 121.69, 111.06 (Ar carbons of ligand), 84.27 (CH of benzene), 40.14 ($N(CH_3)_2$), ESI-MS: shows a peak at m/z 481.0804 $[M\text{-}Cl]^+$ (calcd m/z 481.0494). Single crystals suitable for X-ray diffraction study were procured under slow evoporation of CH_2Cl_2 in petroleum ether solution.

[Ru(L2)(η^6-C_6H_6)Cl] (**2**). Brown solid. Yield = 78%, m.p.: 189 °C (with decomposition); calculated: $C_{22}H_{21}N_3Cl_2ORu$: C, 51.22; H, 4.17; N, 8.17%. Found: C, 51.27; H, 4.11; N, 8.15%. IR (KBr, cm^{-1}): 1523 $\nu_{(C=N-N=C)}$, 1366 $\nu_{(C-O)}$. UV-Vis (CH_3CN, λ_{max}/nm) (ε_{max}/dm^3 mol^{-1} cm^{-1}): 389(2654), 291(5510), 233(10700). ^{1}H NMR (400 MHz, $CDCl_3$) (δ ppm): 8.80

(s, 1H, HC=N), 6.68–8.00 (m, 8H, Ar), 5.37 (s, 6H, CH-benzene), 3.01 (s, 6H, $N(CH_3)_2$). ^{13}C NMR (100 MHz, $CDCl_3$, δ, ppm): 172.18 (C─O), 161.37 (C═N), 151.80 (C-$N(CH_3)_2$), 136.23, 132.23, 130.04, 128.06, 121.44, 111.06 (Ar carbons of ligand), 84.28 (CH of benzene), 40.14 ($N(CH_3)_2$), ESI-MS: shows a peak at m/z 516.0173 $[M+H]^+$ (calcd m/z 515.0105).

[Ru(L3)(η^6-C_6H_6)Cl] (**3**). Brown solid. Yield = 81%, m.p.: 202 °C (with decomposition); calculated: $C_{23}H_{24}N_3O_2ClRu$: C, 61.32; H, 4.08; N, 4.93%. Found: C, 61.34 H, 4.04; N, 4.95%. IR (KBr, cm^{-1}): 1523 $\nu_{(C=N-N=C)}$ 1342 $\nu_{(C-O)}$. UV-Vis (CH_3CN, λ_{max}/nm) (ε_{max}/dm^3 mol^{-1} cm^{-1}): 387(2114), 293(5649), 233(10611). ^1H NMR (400 MHz, $CDCl_3$) (δ ppm): 8.85 (s, 1H, HC=N), 6.75–8.06 (m, 8H, Ar-H of ligand), 5.42 (s, 6H, CH-benzene), 3.07 (s, 6H, $N(CH_3)_2$), 3.82 (s, 3H, OCH_3). ^{13}C NMR (100 MHz, $CDCl_3$, δ, ppm): 173.21 (C─O), 161.28 (C═N), 151.62 (C-$N(CH_3)_2$), 132.19, 130.28, 124.71, 121.91, 113.12, 111.06 (Ar carbons of ligand), 84.24 (CH of benzene), 55.29 (OCH_3) 40.12 ($N(CH_3)_2$), ESI-MS: shows a peak at m/z 511.0908 $[M-Cl]^+$ (calcd m/z 511.0600).

[Ru(L1)(η^6-*p*-cymene)Cl] (**4**). Red-Brown solid. Yield = 85%, m.p.: 210 °C (with decomposition); calculated: $C_{26}H_{30}N_3OClRu$: C, 64.47; H, 5.24; N, 4.70%. Found: C, 64.49; H, 5.26; N, 4.68%. IR (KBr, cm^{-1}): 1523 $\nu_{(C=N-N=C)}$, 1354 $\nu_{(C-O)}$. UV-Vis (CH_3CN, λ_{max}/nm) (ε_{max}/dm^3 mol^{-1} cm^{-1}): 387(2513), 294(6140), 231(11460). ^1H NMR (400 MHz, CDCl3) δ (ppm): 8.88 (s, 1H, HC=N), 6.74–8.08 (m, 9H, Ar), 5.43 (d, J = 6 Hz, 1H, p-cym-H), 5.34 (d, J = 6 Hz, 1H, p-cymene-H), 4.96 (d, J = 6.4 Hz, 1H, p-cymene-H), 4.72 (d, ^3J = 6 Hz, 1H, p-cymene-H), (3.07, s, 6H, -$N(CH_3)_2$), 2.67 (m, 1H, p-cym $CH(CH_3)_2$), 2.30 (s, 3H, p-cymene-CCH_3), 1.13 (dd, J = 12.4 Hz, 6H, p-cymene-$CH(CH_3)_2$). ^{13}C NMR (100 MHz, $CDCl_3$, δ, ppm): 173.13 (C─O), 160.30 (C═N), 151.57 (C-$N(CH_3)_2$) 132.31, 129.99, 128.64, 127.76, 122.03, 111.09 (Ar carbons of ligand), 101.42 and 101.13 (quaternary carbons of *p*-cymene), 80.97, 81.39, 82.11, 84.62 (Ar carbons of *p*-cymene), 40.12 ($N(CH_3)_2$), 30.91 (CH, *p*-cymene), 22.60, 22.02 ($2CH_3$, *p*-cymene), 18.90 (CH_3, *p*-cymene), ESI-MS: shows a peak at m/z 538.1190 $(M+H)^+$(calcd m/z 537.1120). Single crystals suitable for X-ray diffraction study were procured under slow evoporation of CH_2Cl_2 in petroleum ether solution.

[Ru(L2)(η^6-*p*-cymene)Cl] (**5**). Red-Brown solid. Yield = 89%, m.p.: 205 °C (with decomposition); calculated: $C_{26}H_{29}N_3Cl_2ORu$: C, 61.15; H, 4.49; N, 4.46%. Found: C, 61.13; H, 4.53; N, 4.46%. IR (KBr, cm−1): 1519 $\nu_{(C=N-N=C)}$, 1346 $\nu_{(C-O)}$. UV-Vis (CH_3CN, λ_{max}/nm) (ε_{max}/dm^3 mol^{-1} cm^{-1}): 388(1457), 287(5564), 236(10096). ^1H NMR (400 MHz, $CDCl_3$) δ

(ppm): 8.85 (s, 1H, HC=N), 6.74–8.03 (m, 8H, Ar-H of ligand), 5.42 (d, J = 5.6 Hz, 1H, p-cymene-H), 5.33 (d, J = 5.6 Hz, 1H, p-cymene-H), 4.96 (d, J = 5.6 Hz 1H, p-cymene-H), 4.72 (d, J = 5.6 Hz, 1H, p-cymene-H), (3.07, s, 6H, -N(CH_3)$_2$), 2.64 (m, 1H, p-cymene-CH(CH_3)$_2$), 2.30 (s, 3H, p-cymene-CCH_3), 1.11-1.13 (dd, J = 12 Hz, 6H, p-cymene-CH(CH_3)$_2$). ^{13}C NMR (100 MHz, $CDCl_3$, δ, ppm): 171.99 (C═O), 160.66 (C═N), 151.63 (C-N(CH_3)$_2$), 135.92, 132.34, 130.97, 130.04, 127.95, 121.81, 111.08 (Ar carbons of ligand), 101.52 and 101.15 (quaternary carbons of *p*-cymene), 84.57, 82.14, 81.30, 80.90 (Ar carbons of *p*-cymene), 40.15 (N(CH_3)$_2$), 30.92 (CH, *p*-cymene), 22.62, 21.95 (2CH_3, *p*-cymene), 18.91 (CH_3, *p*-cymene). ESI-MS: shows a peak at m/z 572.0800 $(M+H)^+$(calcd m/z 571.0712).

[Ru(L3)(η^6-*p*-cymene)Cl] (**6**). Red-Brown solid. Yield = 90%, m.p.: 196 °C (with decomposition); calculated: $C_{27}H_{32}N_3O_2ClRu$: C, 63.50; H, 5.01; N, 4.49%. Found: C, 63.48; H, 5.01; N, 4.48%. IR (KBr, cm^{-1}): 1508 $\nu_{(C=N-N=C)}$, 1356 $\nu_{(C-O)}$. UV-Vis (CH_3CN, λ_{max}/nm) (ε_{max}/dm^3 mol^{-1} cm^{-1}): 385(1222), 290(5975), 234(16589). ^{1}H NMR (400 MHz, $CDCl_3$) δ (ppm): 8.86 (s, 1H, HC=N), 6.75–8.03 (m, 8H, Ar), 5.42 (d, J = 6 Hz, 1H, p-cymene-H), 5.33 (d, J = 5.6 Hz, 1H, p-cymene-H), 4.95 (d, J = 6 Hz, 1H, p-cymene-H), 4.69 (d, ^3J = 6 Hz, 1H, p-cymene-H), (3.07, s, 6H, -N(CH_3)$_2$), 3.81 (s, 3H, OCH3), 2.67 (m, 1H, p-cymene-CH(CH_3)$_2$), 2.29 (s, 3H, p-cymene-CCH_3), 1.15 (dd, J = 13.2 Hz 6H, p-cymene-CH(CH_3)$_2$). ^{13}C NMR (100 MHz, $CDCl_3$, δ, ppm): 173.01 (C═O), 161.16 (C═N), 151.48 (C-N(CH_3)$_2$), 132.24, 130.29, 125.02, 122.28, 113.06, 111.11 (Ar carbons of ligand), 101.39 and 101.02 (quaternary carbons of *p*-cymene), 84.63, 82.08, 81.39, 80.94 (Ar carbons of *p*-cymene), 55.27 (OCH_3), 40.17 (N(CH_3)$_2$), 30.91 (CH, *p*-cymene), 22.63, 22.00 (2CH_3, *p*-cymene), 18.89 (CH_3, *p*-cymene). ESI-MS: shows a peak at m/z 568.1295 $(M+H)^+$ (calcd m/z 567.1226).

Cell culture

A549, LoVo and HuH-7cells were purchased from the cell bank of the Chinese Academy of Sciences (Shanghai, China). A549 and LoVo cells were cultured in RPMI-1640 (Gibco) supplemented with 10% fetal bovine serum (FBS; Gibco). HuH-7 cells were cultured in Dulbecco's modified Eagle's medium (DMEM) containing 10% FBS and 1% nonessential amino acids. All cells were maintained at 37 °C in 5% CO_2.

EdU assay

2×10^4 of A549 cells were seeded into 48-well plates with per well and hatched at 37 °C under a 5% CO_2 atmosphere for 24 h. Complexes **4-6** and cisplatin(3.5 μM, equiv concentrations)were then added to the cells and incubated for an additional 24 h at 37 °C. At the end of the drug treatment DNA synthesis were measured using Alexa Fluor 488 Assay Kit (Invitrogen)Click-iT EdU. Click-iT EdU added and incubated 2 h at room temperature. After the A549 cells were fixed with 4% formaldehyde for 15 min, then 0.5% Triton X-100 was added into the A549 cells and incubated with 10 min. Later, azide labeled Alexa Fluor 488 was added into the A549 cells and incubated 30 min at dark condition. After 30 min later, staining the nuclei with Hoechst 33342 (Invitrogen) for 15 min, the cells were imaged using fluorescence microscopy (Olympus, IX71).

Acridine orange-ethidium bromide (AO-EB) staining

4×10^3 of A549 cells were seeded in 24-well plates and incubated at 37 °C for 24 h. Complexes **4-6** and cisplatin (3.5 μM, equiv concentrations) were incubated with A549 cells. After incubation24 h, AO (100 μg/mL) and EB (100 μg/mL) was added to each well (500 μL). After 5 min later, the cells were imaginedvia a fluorescence microscope (Olympus, BX-60, Japan), and the cell death were measured three random fields of the microscope.

Flow cytometry/Annexin V-PI staining

The flow cytometry analysis with the fluoresceinisothiocyanate (FITC) Annexin V Apoptosis Detection Kit (Multi Sciences, China) used to determine the A549 cells apoptotic ratio. The cells were composed by trypsinization, and washed with twice and resuspended in 500 μL 1 × binding buffer with 5 μL of FITC Annexin V and 10 μL of PI. After 15 min, the samples were subjected to analysis by flow cytometry. The outcomes were analysed with the BD FACS Calibur™ system.

Cell cycle analysis

A549 cells were seeded into 6 well plates incubated, and allowed to attach for 24 h. Then, fresh media containing 3.5 μM complexes **4-6** and cisplatin were added and further incubated for another 24 h. The untreated cells were included as the control. After drug treatment, the cells were centrifuged at 1000 RPM for 5 min and washed with cold PBS. The

cells were fixed with 75% ethanol at 4 °C overnight. The cells were then collected and washed twice with PBS. Thereafter, the cells were stained with a solution containing PI (50 µg/mL) and incubated 30 minin the dark condition. Cell cycle distribution was then analysed with a BD FACSCanto™ II flow cytometer.

3. Results and Discussions

Synthesis and characterization of benzhydrazone ligands and their arene Ru(II) complexes

The hydrazone ligand and its derivatives were easily prepared in an excellent yield by the condensation of 4-dimethylamino benzaldehyde with substituted benzhydrazides in an equi-molar ratio and were confirmed by NMR (supplementary information, ESI S6-S8). Metallation was accomplished by reacting the ruthenium(II) arene precursors [(η^6-arene)RuCl(µ-Cl)]$_2$ (arene-benzene or *p*-cymene) and prepared hydrazones in 1:2 molar ratio in the presence of Et_3N base (Scheme 1). All the new complexes **1-6** (Figure 2) of the general formula, [(η^6-arene)Ru(L)Cl], L= substituted dimethylamino benzhydrazone derivatives) were collected in good yields. The coordination of the imidolate oxygen to the ruthenium(II) ion was facilitated by the addition of Et_3N to the reaction mixture. All complexes were found to be air-stable and were soluble in most organic solvents.

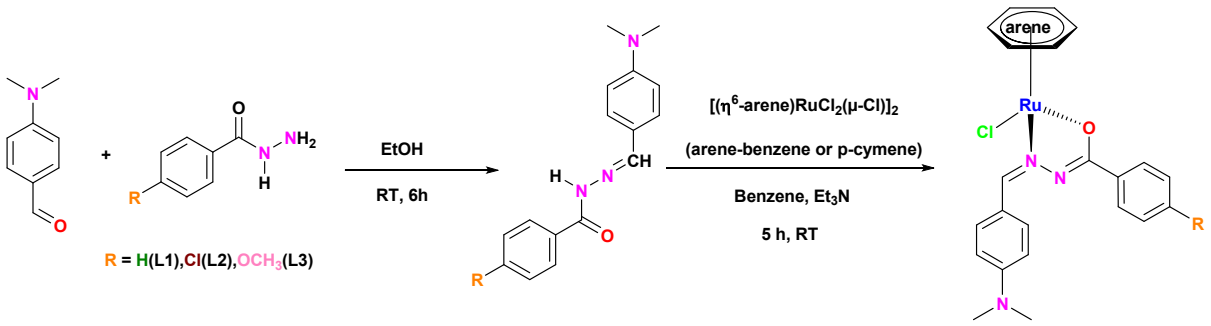

Scheme 1: Synthesis of benzhydrazone ligands and their arene Ru(II) complexes.

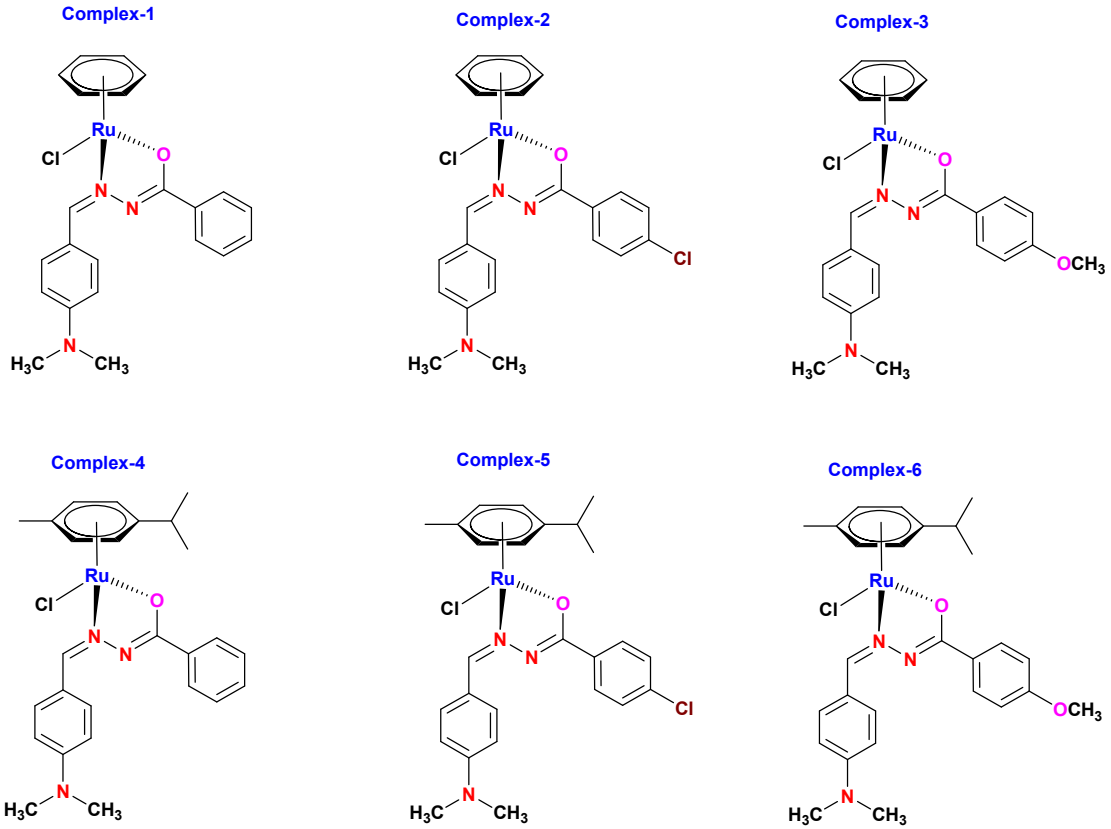

Figure 2. Chemical structures of arene Ru(II) benzhydrazone complexes **1-6.**

A medium to strong band was observed in the region 3225-3280 cm^{-1} characteristic to N-H functional group of the free ligand. Further, ligands displayed -CH=N and C=O absorptions in the region 1546-1601 cm^{-1} 1653-1661 cm^{-1} respectively, indicated that the ligand exists in amide form in solution free state. Upon complexation, the bands due to N-H and C=O stretching vibrations were disappeared denoted that the ligand underwent tautomerization and subsequent coordination in imidol form which was further supported by the emergence of new band C-O-Ru in 1340-1370 cm^{-1}. Coordination of the azomethine nitrogen of the ligand to the Ru(II) ion was corroborated by the reduction of the electron density on azomethine link and thus lowering the absorption frequency after complexation (1500-1530 cm^{-1}). Hence the ligand was coordinated to metal *via* imine nitrogen and imidolate oxygen atoms.

The binding of the ligand to metal in the new arene Ru(II) benzhydrazone complexes was further supported by the ^{1}H-NMR spectra (supplementary information ESI, S9-S14) of the new complexes. All the complexes showed multiplets in the region δ 6.68- 8.10 ppm and those have been assigned to the aromatic protons of benzhydrazone ligands. The appearance of a sharp singlet in the region 8.80-8.88 ppm was due to the azomethine proton. The down field shift of the azomethine proton signal C**H**=N in the complexes suggested the deshielding

of the azomethine moiety due to its coordination to ruthenium. The -NH protons of the ligands appeared as a sharp singlet in the region δ 10.29-11.55 ppm and were disappeared after complexation. Aromatic protons of the *p*-cymene ring were observed as doublets at 4.68-5.43 ppm for the complexes **4-6**. Complexes **3** and **6** exhibited methoxy signals of the benzhydrazone ring as singlets around 3.80 ppm. In addition, the two isopropyl methyl protons of the *p*-cymene appeared as doublet of doublet in the region of δ 1.11-1.15 ppm and the isopropyl protons came in the region of δ 2.29-2.67 ppm as septet. Further, the aromatic protons of benzene moiety in the complexes **1-3** displayed an upfield shift of singlet in the region δ 5.37-5.44 ppm. The ^{1}H-NMR spectral data clearly indicated that the coordination of the ligand to ruthenium(II) ion took place *via* the azomethine nitrogen and the imidolate oxygen of the ligands.^{13}C NMR of the complexes showed resonances in the expected region (Figure S13–S18). The upfield shift of the imine carbon (–C=N–) (160.28-161.37 ppm) of the complexes relative to the free ligands (148.00-149.88 ppm) indicated the coordination of the imine nitrogen to the ruthenium centre. Further, the downfield shift of the imidolate carbon (–NH–C=O) from 171.99-173.31 ppm in the free ligand to 161.60-164.34 ppm in the complexes denoted the reduction of the bond order (–N=C–O) upon coordination.

The absorption spectra of all the arene Ru(II) benzhydrazone complexes were recorded in methanol in the range 200-800 nm at room temperature and three bands were observed with absorption maxima in the region 230–389 nm. The two high intensity bands of ligand based transitions (π-π* and n-π*) were detected around 287-294 nm. A relatively intense absorption bands in the region 383-389 nm are attributed to metal to ligand charge transfer bands (MLCT). The pattern of the electronic absorption spectra of all the complexes looks akin to other reported octahedral arene ruthenium(II) benzhydrazone complexes.[29]

Stability studies and HR-MS

The determination of stability of metal complexes in aqueous media is an essential study for the development drug in clinical investigations. The stability of ruthenium complexes in aqueous solution was measured over various time intervals using UV-visible spectrophotometry. The complexes were taken in dimethylsulfoxide and the stock solutions were diluted using aqueous phosphate buffer, at p^{H} 7.4, and finally made to 1×10^{-3} M concentration. The electronic spectra of these complexes were recorded for different time intervals at room temperature and representative spectra were given in supplementary information ESI, S21. It has been observed from the spectral diagram that there was no

significant change over 72 h intervals. Further, the formation of the complexes has been established by ESI-MS spectral studies and the measurements were carried out under positive ion ESI mode using acetonitrile as the solvent. HRMS spectra of complexes **1-6** (supplementary information ESI, S15-S20) displayed peaks at m/z 481.08, 516.01, 511.09, 538.11, 572.08 and 568.12 respectively confirmed the presence of expected moiety in solution phase.

X-ray crystallographic studies

Single crystals of two of the complexes **1** and **4** were isolated by the slow evaporation of the 1:2, CH_2Cl_2: petroleum ether mixture at room temperature and their molecular structures were resolved by single-crystal X-ray diffraction. Details on crystallographic data with refinement parameters and selected bond lengths, bond angles were gathered in Table 1 and Table 2 respectively (supplementary information ESI, S4, S5). From the lattice constants and angles between the primitive lattice vectors, it was obvious that the crystal system of complex **1** was orthorhombic belonging to P b c a space group and **4** was monoclinic fit in with P 21/c space group. The ORTEP view of the complexes **1** and **4** were shown as thermal ellipsoids in Figures **3** and **4** respectively, which clearly indicated that the ligand was chelated to ruthenium ion via the imine nitrogen and imidolate oxygen with the formation of a five-member metallacycle with bite angles 76.73(12) - 76.74(9)° in a piano stool geometry. While the seat of the piano-stool was made by the arene ring, the N^O bidentate benzhydrazone and Cl ligands fashioned the three legs of the stool. Therefore, the ruthenium(II) ion was nested in NOCl(η^6-arene) coordination environment. In both the complexes, the arene ring and ruthenium ion were seated away from the chloride ion which is evident from the bond angles $Centroid_{metallacycle}$-Ru-$Centroid_{benzene}$ = 89.21°; $Centroid_{benzene}$-Ru-Cl = 127.56°; $Centroid_{metallacycle}$-Ru-$Centroid_{cymene}$ = 86.25°; $Centroid_{cymene}$-Ru-Cl = 129.82°. The stool top arene is π bonded to the Ru ion with average Ru-C bond length 2.172-2.196 Å. The σ bond lengths of three legs of the stool, Ru-N, Ru-O and Ru-Cl and bond angles were tantamount with other structurally related benzene and *p*-cymene ruthenium complexes encompassing similar piano stool ruthenium complexes.[30]

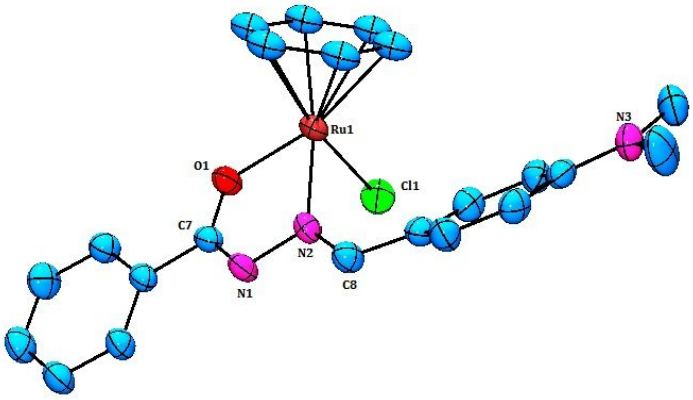

Figure 3. The ORTEP diagram of the complex **1** with 30% probability.

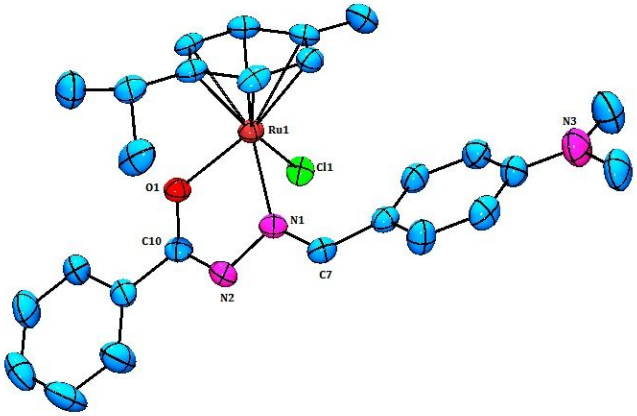

Figure 4. The ORTEP diagram of the complex **4** with 30% probability.

***In vitro* cytotoxic activity by MTT assay**

To check the potency of the complexes in inhibiting the growth of cancer cells, MTT assay was performed with A549 (Lung carcinoma), LoVo (Colon adenocarcinoma) and HuH-7 (Hepato cellular carcinoma) cells. There was no inhibition of the cell growth even up to 100 μM using the free ligands and ruthenium precursors. Hence, the observed cytotoxicity of the complexes was due to chelation. As shown in Table 2, most of the complexes exhibited high potent cytotoxicity against the tested cancer cells. Among the three cancer cells screened, the complexes showed superior activity in inhibiting the growth of A549 lung cancer cells. It is evident from the IC_{50} values that the complexes comprising methoxy group have some marked effect on inhibition of cancer cell growth (Figure 5). Gratifyingly, complexes **4-6** outperformed the anticancer activity of cisplatin and two-fold enhanced activity was found against LoVo and HuH cells in case of complex **6.** [31-33] When scrutinizing the results, it was found that the complexes containing *p*-cymene moiety displayed significant effect when compared to complexes **1-3** which contain benzene moiety, implied the strong hydrophobic interaction of Ru(II)-cymene complexes with the cell membrane.[26] This observation highlighted the impact of arene moiety in antiproliferation. Gratifyingly, the cancer cell growth inhibition capability of the titled complexes was significantly high when compared to other arene ruthenium complexes found in the literature as evidenced by the low IC_{50} values.[34,35]

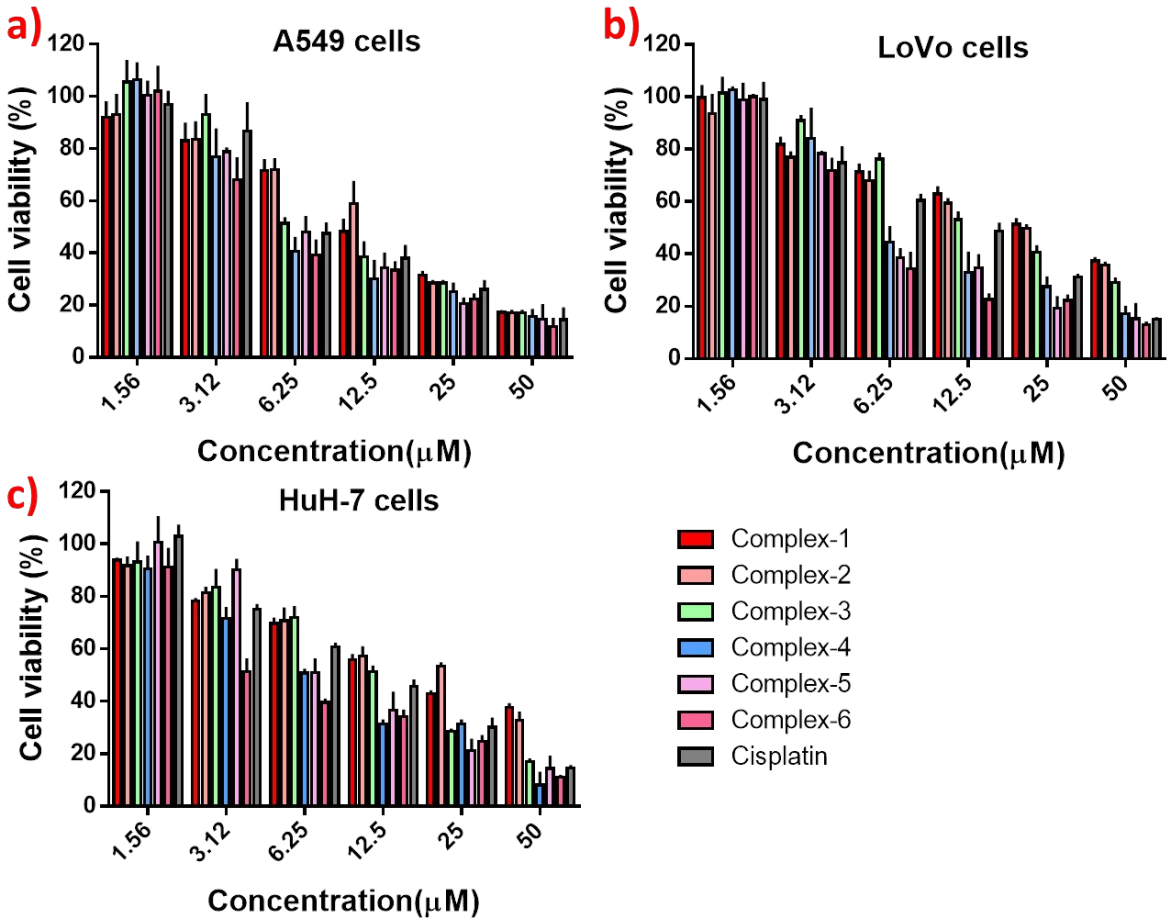

Figure 5. *In vitro* cytotoxicity in (**a**) A549 cells, (**b**) LoVo cells and (**c**) HuH-7 cells after 72-h treatment with complexes **1**-**6** and cisplatin.

Table 1. Antitumor potential of arene Ru(II) benzhydrazone complexes after 72 h of incubation (expressed as IC_{50}±SD in μM).[a]

Cell line	A549	LoVo	HuH-7
Complex-1	12.63 ± 0.49	25.04 ± 1.83	19.74 ± 1.12
Complex-2	13.85 ± 0.77	21.91 ± 1.55	22.14 ± 1.37
Complex-3	9.92 ± 0.98	17.88 ± 1.03	12.78 ± 0.51
Complex-4	7.15 ± 0.78	8.21 ± 0.86	7.43 ± 0.48
Complex-5	7.73 ± 0.58	6.92 ± 0.61	8.74 ± 0.68
Complex-6	6.52 ± 0.69	5.62 ± 0.49	5.37 ± 0.56
Cisplatin	8.72 ± 0.74	10.95 ± 0.67	10.68 ± 0.68

[a] Determined by MTT assay. IC_{50} values indicated the concentrations of complexes **1**-**6** and cisplatin required to inhibit 50% of cell growth with respect to control groups. The data obtained were

based on the average of three independent experiments, and the reported errors were the corresponding standard deviations.

Antiproliferative activity by Edu assay

Further, 5-ethynyl-2′-deoxyuridine (EdU) incorporation assay was performed to evaluate the effect of complexes **4-6** and cisplatin on prohibiting the cancer cell proliferation. The EdU is a nucleoside module of thymidine that is incorporated into DNA only during DNA replication allowing the visualization of newly synthesized DNA by "click" chemistry through its reaction of terminal alkyne group with fluorescent azides. The percentage of EdU-stained cells was calculated on the basis of five randomly selected fields for each group after treatment with complexes **4-6** and cisplatin (3.5 μM, equiv concentrations) for 24 h. After the treatment of the complexes, it has been observed that the percentage of cell proliferation was significantly decreased (Figure 6). These results suggested that the complexes notably inhibited the growth of A549 cells cell lines. Complex **6** exhibited higher antiproliferation which may be due to the presence of electron-donating methoxy group that subsequently increases the lipophilic character of the metal complex and thus influences its permeation through the lipid layer of the cell membrane.

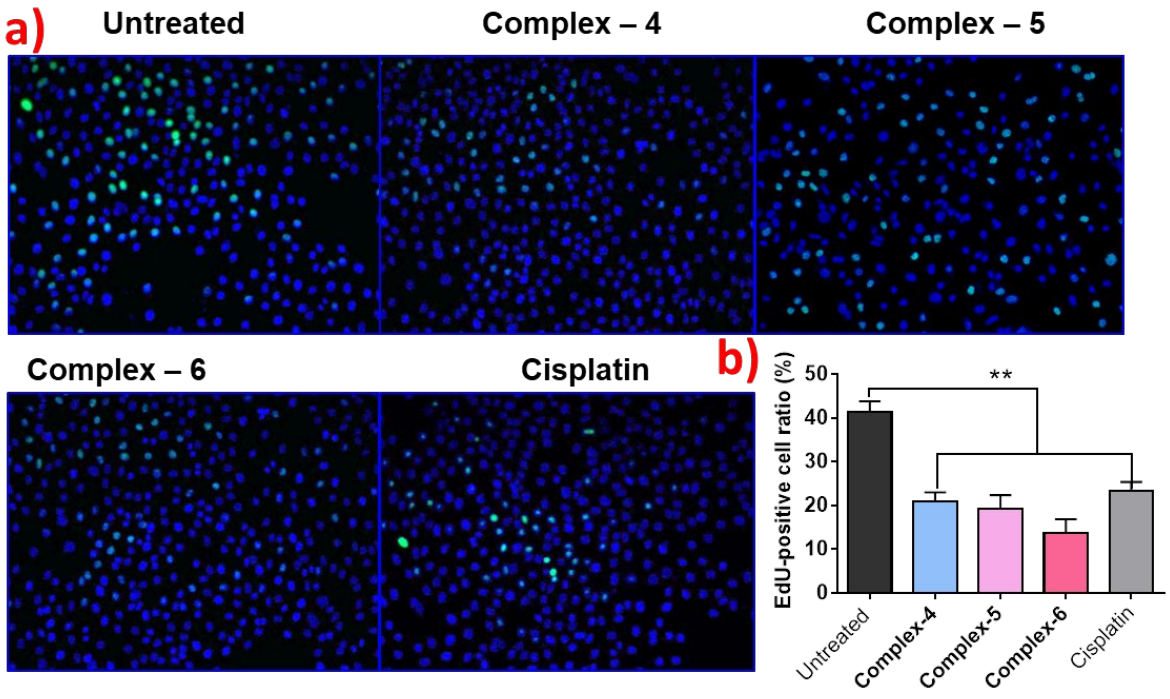

Figure 6.a) A Click-iT EdU assay for determining the proliferation of A549 cells. The cells were treated with complexes **4-6** and cisplatin(3.5 μM, equiv concentrations) for 24 h. b) Quantification of

cell proliferation. The data are presented as the means ± s.d.; n≥5 regions with a total of 1500-2000 cells analyzed; **$p<0.01$.

Apoptosis induction by dual AO-EB fluorescent staining

AO-EB staining method is generally used to observe the apoptosis inducing property of metal complexes. Cells undergoing apoptosis was monitored by morphological changes like cytoplasmic shrinkage, membrane blebbing and nuclear condensation. A549 cell were stained by acridine orange and ethidium bromide, following 24 h incubation with complexes **4-6**. AO dye can stain both live and dead cells and shows green fluorescence. EB only stains cells that have lost their membrane integrity and exhibits red fluorescence. Necrotic cells are stained in red but have nuclear morphologies that resemble those of viable cells. As shown in Figure 7, the A549 cells treated with complexes **4-6** and cisplatin showed red orange fluorescence with fragmented chromatin, suggesting that the complexes **4-6** largely induced apoptosis in A549 cells.[36]

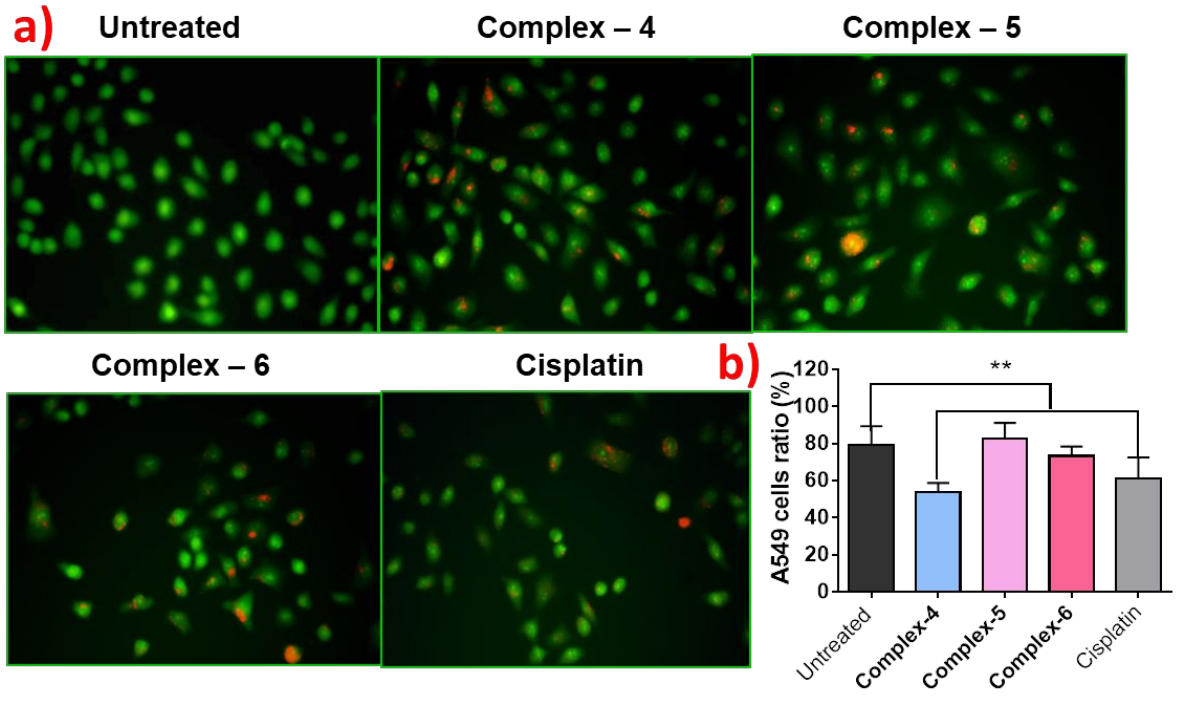

Figure 7.a) Dual AO/EB fluorescent staining of A549 cells after treatment with complexes **4-6** and cisplatin(3.5 μM, equiv concentrations) for 24 h. b) Cell death rates in AO/EB staining were quantified. The data are presented as the means ± s.d.; n≥5 regions with a total of 1500-2000 cells analyzed; **$p<0.01$.

Apoptosis evaluation by flow cytometry

The induction of apoptotic cell death by complexes **4-6** was further investigated by Alexa Fluor 488 Annexin V/propidium iodide (PI) double-staining assay in A549 cells along with cisplatin (Figure 8a). Fluorescently labelled Annexin V is used to identify the presence of phosphatidylserine on the outer leaflet of the cell membrane during apoptosis.[37] Different degrees of apoptosis have been observed when the cancer cells were exposed to complexes **4-6** and cisplatin. The lower left quadrant expresses the viable cells while the lower right and upper right quadrants indicate early and late apoptotic cells, respectively. The percentage of apoptotic cells in each group is shown in the Figure 8b. From the results, it was found that, the complexes significantly brought out apoptosis when compared to cisplatin.

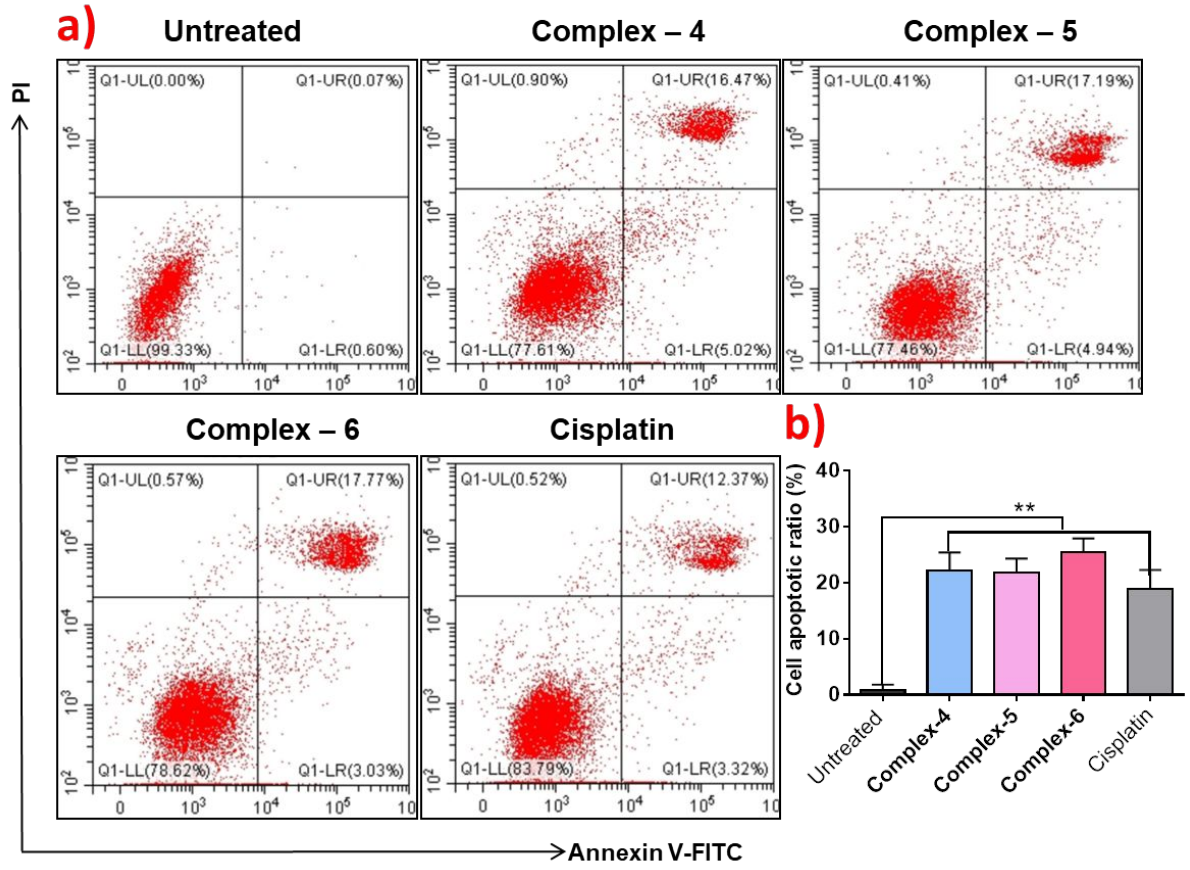

Figure 8. The concentrations of complexes **4-6** and cisplatin(3.5 μM, equiv concentrations) for 24 h. (**a-b**) Apoptosis of A549 cells after treatment with compounds was determined by an Alexa Fluor 488 Annexin V/propidium iodide (PI) double-staining assay. The apoptotic ratio is shown in the upper panel, and the quantitative results are shown in the lower panel.

Cell-cycle analysis by flow cytometry

Deregulated cell-cycle control is a fundamental aspect of cancer, and the process is related to the proliferation and death of cancer cells.[38] Consequently, the effect of complexes on cell cycle progression was examined using FACS. Upon exposure of A549 cells to drugs at a 3.5 μM concentration for 24 h, the percentage of cells in the G0/G1 phase decreased from 65.5% to 14.5%, 14.1%, 13.6% and 15.2% for complexes **4-6** and cisplatin, respectively (Figure 9). Especially, complexes **4-6** elicited a strong S phase arrest in cells, accounting for 83.3%, 86.7% and 87.3% of the cell population, respectively (untreated cells, 27.9%). Thus, the enrichment of the S phase arrest of cancer cells may result in apoptosis by disrupting the cell cycle.

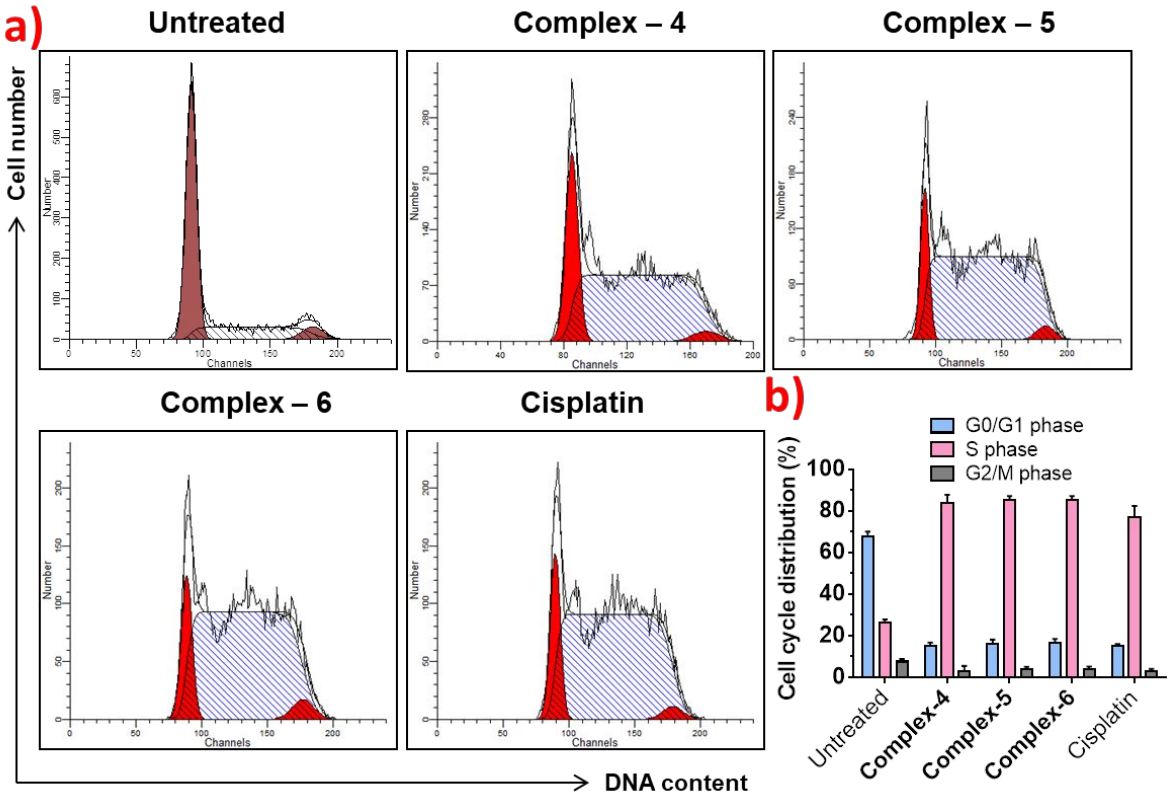

Figure 9. The a**)** A549 cells were treated with complexes **4-6** and cisplatin(3.5 μM, equiv concentrations) for 24 h and then fixed and stained with propidium iodide. A representative picture is presented. **b)** The histogram shows the distribution of the cell cycle, indicating that complexes **4-6** mainly arrested cells at the S phase arrest.

4. CONCLUSIONS

In an attempt of inventing ruthenium anticancer drug, a set of new half-sandwich arene ruthenium(II) complexes bearing N,N-dimethylamino benzhydrazone have been isolated. The composition of the complexes was established by analytical, IR, UV-vis, NMR and HR-MS methods. Single crystal X-ray diffraction study of complexes confirmed the bidentate chelation of benzhydrazone ligands and revealed the presence of pseudo- octahedral geometry around ruthenium ion. *In vitro* cytotoxic activity studies attested that the complexes are potent in cancer cell growth inhibition. In particular, the *p*-cymene complexes **4-6** outperformed the benzene complexes **1-3** and cisplatin concluding the impact of arene moiety in anticancer activity. Further, the desirable apoptotic cell death mechanism of the complexes determined by various assays suggested that the arene ruthenium benzhydrazones may be a perfect pathway of finding out more efficient medicines to the gallery of ruthenium anticancer drugs.

Acknowledgement

We express sincere thanks to DST–FIST, New Delhi, for the use of HR-MS and Bruker 400 MHz facilities at the School of Chemistry, Bharathidasan University, Tiruchirappalli. M.S.Khan gratefully acknowledges Zhejiang province fund (No. 519000-X81801) for the financial support.

Conflict of interest

The authors declare no potential conflicts of interest.

References

1. L. Kelland, *Nature Reviews Cancer,* 2007, **7**, 573-584.

2. I. Judson, T. Cerny, R. Epelbaum, D. Dunlop, J. Smyth, B. Schaefer, M. Roelvink, S. Kaplan and A. Hanauske, *Annals of Oncology,* 1997, **8**, 604-606.

3. P. Koepf-Maier and H. Koepf, *Chemical Reviews,* 1987, **87**, 1137-1152.

4. K. Irena, *Curr Med Chem,* 2006, **13**, 1085-1107.

5. E. Reisner, V. B. Arion, B. K. Keppler, A. J. L. Pombeiro, *Inorganica Chimica Acta,* 2008, **361**, 1569-1583.

6. B. Bernhard, *Mini-Reviews in Medicinal Chemistry,* 2016, **16**, 804-814.

7. A. Bergamo, C. Gaiddon, J. H. M. Schellens, J. H. Beijnen and G. Sava, *J. Inorg Biochem* 2012, **106**, 90-99.

8. A. Bergamo and G. Sava, *Dalton Transactions,* 2011, **40**, 7817-7823.

9. (a) C. G. Hartinger, S. Zorbas-Seifried, M. A. Jakupec, B. Kynast, H. Zorbas and B. K. Keppler, *J. Inorg. Biochem.,* 2006**, 100**, 891-904. (b) C. G. Hartinger, M. A. Jakupec, S. Zorbas-Seifried, M. Groessl, A. Egger, W. Berger, H. Zorbas, P. J. Dyson and B. K. Keppler, *Chemistry & Biodiversity,* 2008, **5**, 2140-2155.

10. (a) A. Bergamo, L. Messori, F. Piccioli, M. Cocchietto and G. Sava, *Invest. New Drugs,* 2003, **21**, 401-411. (b) E. Alessio, G. Mestroni, A. Bergamo and G. Sava, *Curr. Top. Med. Chem.* 2004, **4**, 1525-1535.

11. L. Zeng, P. Gupta, Y. Chen, E. Wang, L. Ji, H. Chao and Z. S. Chen, *Chem. Soc. Rev.* 2017, **46,** 5771-5804.

12. D. A. Smithen, H. Yin, M. H. R. Beh, M. Hetu, T. S. Cameron, S. A. McFarland and A. Thompson, *Inorg. Chem.,* 2017, **56**, 4121-4132.

13. R. L. Hayward, Q. C. Schornagel, R. Tente, J. S. Macpherson, R. E. Aird, S. Guichard, A. Habtemariam, P. Sadler and D. I. Jodrell, *Cancer Chemother. Pharmacol.,* 2005, **55**, 577-583.

14. S. Chatterjee, S. Kundu, A. Bhattacharyya, C.G. Hartinger and P. J. Dyson, *Journal of Biological Inorganic Chemistry,* 2008, **13**, 1149-1155.

15. R. E. Morris, R. E. Aird, P. del Socorro Murdoch, H. Chen, J. Cummings, N. D. Hughes, S. Parsons, A. Parkin, G. Boyd, D. I. Jodrell and P. J. Sadler, *J. Med. Chem.,* 2001, **44**, 3616-3621.

16. P. Zhang and P. J. Sadler, *Journal of Organometallic Chemistry,* 2017, **839**, 5-14.

17. S. Grgurić-Šipka, I. Ivanović, G. Rakić, N. Todorović, N. Gligorijević, S. Radulović, V. B. Arion, B. K. Keppler and Ž. L. Tešić, *Eur J Med Chem.,* 2010, **45**, 1051-1058.

18. F. Martínez-Peña, S. Infante-Tadeo, A. Habtemariam and A. M. Pizarro, *Inorg Chem* 2018, **57**, 5657-5668.

19. R. Pettinari, F. Marchetti, C. Di Nicola, C. Pettinari, A. Galindo, R. Petrelli, L. Cappellacci, M. Cuccioloni, L. Bonfili, A. M. Eleuteri, M. F. C. Guedes da Silva and A. J. L. Pombeiro, *Inorg Chem,* 2018, **57,** 14123-14133.

20. F.-U. Rahman, M. Z. Bhatti, A. Ali, H.-Q. Duong, Y. Zhang, X. Ji, Y. Lin, H. Wang, Z.-T. Li and D.-W. Zhang, *Eur. J. Med Chem,* 2018, **157**, 1480-1490.

21. U. Ndagi, N. Mhlongo, M. E. Soliman, in *Drug Des Devel Ther, Vol. 11*, 2017, pp. 599-616.

22. K. T. Hufziger, F. S. Thowfeik, D. J. Charboneau, I. Nieto, W. G. Dougherty, W. S. Kassel, T. J. Dudley, E. J. Merino, E. T. Papish, J. J. Paul, *J. Inorg Biochem.,* 2014, **130**, 103-111.

23. Y. K. Yan, M. Melchart, A. Habtemariam and P. J. Sadler, *Chemical Communications* **2005**, 4764-4776.

24. N. G. Kandile, M. I. Mohamed, H. Zaky and H. M. Mohamed, *Eur J Med Chem* 2009, **44**, 1989-1996.

25. K. Hruskova, P. Kovarikova, P. Bendova, P. Haskova, E. Mackova, J. Stariat, A. Vavrova, K. Vavrova and T. Simunek, *Chem Res Toxicol,* 2011, **24**, 290-302.

26. M. S. Mohamed Kasim, S. Saranya and R. Rengan, *Inorganic Chemistry Frontiers,* 2018, **5**, 585-596.

27. I. G. Ribeiro, K. C. M. da Silva, S. C. Parrini, A. L. P. de Miranda, C. A. M. Fraga, E. J. Barreiro, *Eur J Med Chem.,*1998, **33**, 225-235.

28. P. C. Lima, L. M. Lima, K. C. M. da Silva, P. H. O. Léda, A. L. P. de Miranda, C. A. M. Fraga and E. J. Barreiro, *Eur.J.Med.Chem.,* 2000, **35**, 187-203.

29. (a) M. K. M. Subarkhan and R. Ramesh, *Inorganic Chemistry Frontiers,* 2016, **3**, 1245-1255. (b) R. Pettinari, F. Marchetti, C. D. Nicola, C. Pettinari, A. Galindo, R. Petrelli, L. Cappellacci, M. Cuccioloni, L. Bonfili, A. M. Eleuteri, M. Fátima C. Guedes da Silva and Armando J. L. Pombeiro, *Inorg. Chem*, 2018**, 57(22)**, 14123-14133.

30 (a) N. Mohan, M. K. Mohamed Subarkhan and R. Ramesh, *Journal of Organometallic Chemistry* 2018, **859**, 124-131. b) M. K. Mohamed Subarkhan, R. Ramesh and Y. Liu, *New Journal of Chemistry,* 2016, **40**, 9813-9823. c) D. Pandiarajan and R. Ramesh, *Journal of Organometallic Chemistry,* 2013, **723**, 26-35.

31. É. A. Enyedy, G. M. Bognár, T. Kiss, M. Hanif and C. G. Hartinger, *Journal of Organometallic Chemistry* 2013, **734**, 38-44.

32. R. E. Morris, R. E. Aird, P. del Socorro Murdoch, H. Chen, J. Cummings, N. D. Hughes, S. Parsons, A. Parkin, G. Boyd, D. I. Jodrell and P. J. Sadler, *Journal of Medicinal Chemistry* 2001, **44**, 3616-3621.

33. A. Habtemariam, M. Melchart, R. Fernández, S. Parsons, I. D. H. Oswald, A. Parkin, F. P. A. Fabbiani, J. E. Davidson, A. Dawson, R. E. Aird, D. I. Jodrell and P. J. Sadler, *Journal of Medicinal Chemistry,* 2006, **49**, 6858-6868.

34. J. Ruiz, V. Rodríguez, N. Cutillas, A. Espinosa and M. J. Hannon, *Inorg Chem* 2011, **50**, 9164-9171.

35. L. He, S.-Y. Liao, C.-P. Tan, R.-R. Ye, Y.-W. Xu, M. Zhao, L.-N. Ji and Z.-W. Mao, *Chemistry – A European Journal,* 2013, **19**, 12152-12160.

36. M. Mohamed Subarkhan, R. N. Prabhu, R. Raj Kumar and R. Ramesh, *RSC Advances* **2016**, **6,** 25082-25093.

37. H. Wang, J. Chen, C. Xu, L. Shi, M. Tayier, J. Zhou, J. Zhang, J. Wu, Z. Ye, T. Fang and W. Han, *Theranostics*, 2017,**7(15)**, 3638-3652.

38. Y. Yuan, L. Xu, S. Dai, M. Wang and H. Wang, *Journal of Materials Chemistry B* 2017, **5**, 2425-2435.

The manuscript describes a convenient method of synthesis of a panel of organometallic arene ruthenium(II) complexes bearing dimethylaminobenzhydrazone ligands. The molecular structures of two representative complexes have been confirmed by single crystal X-ray diffraction method. The In vitro cytotoxic activity of the complexes was screened against some human cancer cell lines and the complexes showed lower IC50 values than cisplatin against all the cancer cell lines tested. Furthermore, the inhibition of cancer cell proliferation and apoptosis-inducing properties of the complexes was explored through Edu assay, fluorescence microscopy visualization and flow cytometry. Hence, there is much scope within this class of compounds for the development of promising anticancer drugs.